RSC Advances

ROYAL SOCIETY OF CHEMISTRY

www.rsc.org/advances

Journal Name

RSCPublishing

COMMUNICATION

Enhanced Electroactivity and Substrate Affinity of Microperoxidase-11 Attached to Pyrene-linkers π-π Stacked on Carbon Nanostructure Electrodes

Cite this: DOI: 10.1039/x0xx00000x

Received 00th January 2012,
Accepted 00th January 2012

DOI: 10.1039/x0xx00000x

www.rsc.org/

*K. Sudhakara Prasad, Charuksha Walgama and Sadagopan Krishnan**

An exceptionally large electroactively connected microperoxidase-11 (MP-11) with strong affinity for an organic peroxide and offering a high electrocatalytic reduction current density of 7.5 mA cm^{-2} is achieved for the first time. For this, MP-11 was attached via pyrene linkers on the surface of multiwalled carbon nanotubes-modified graphite electrodes.

The nature of protein arrangement on the surface of electrode plays an important role in controlling the direct electron transfer and catalytic properties.[1-4] Due to this reason, the specific immobilization of metalloenzymes on various functionalized "*nano*" surfaces has gained enormous attention recently. Both the covalent and non-covalent attachment methods have been reported for attaching enzymes to carbon nanostructures for electrocatalytic applications.[5-12]

Among several redox-active proteins attached to nanotube-modified electrodes, MP-11 (an 11-amino acid heme-iron peptide of cytochrome c) has gained enormous interests due to its small size with hydroxylation and peroxidase activities, similar to heme peroxidases and drug-metabolizing cytochrome P450 enzymes.[9,13] Microperoxidases are obtained from the proteolytic digestion of cytochrome c and retain the proximal histidine (His18) ligand of heme with the proximal imidazole coordinated to the heme-iron tightly at neutral pH.[14] The axial coordination of histidine to the ferric-heme has been shown to have a crucial role in the activity of peroxidases.[15,16] Prior studies reported the immobilization of MP-11 on gold surface by self-assembly techniques, simple adsorption and covalent attachment onto carbon nanotubes, and adsorption to nonporous films of indium tin oxide or silica cavity arrays.[9,13-25]

Katz and Willner studied the direct electrochemistry of MP-11 as a self-assembled monolayer on a cystamine-modified gold electrode.[18] Gooding *et al*. examined the MP-11 film bound to the free ends of aligned –COOH functionalized, shortened single-walled carbon nanotubes (SWNT) on the surface of cysteamine-layered gold electrodes.[9] Dong *et al.* used an adsorption approach involving the immersion of MWNT-modified glassy carbon electrodes in MP-11 solution for 10 h.[22] Another study utilized the covalent immobilization of MP-11 onto carbon nanotube structures by ion soft-landing method.[17] However, to our knowledge, the electrocatalytic properties of MP-11 films covalently linked onto pyrenyl carbon-nanostructures have not been investigated yet.

The MP-11 used in this study was the sodium salt of microperoxidase prepared from equine heart cytochrome c by peptic digestion. The direct electrochemistry of MP-11 films on high purity graphite (HPG) electrodes modified with multiwalled carbon nanotubes (MWNT) and π-π stacked with 1-pyrenebutyric acid (MWNT/Py) was investigated by cyclic voltammetry. The covalent attachment of the two MP-11 amine groups (N-terminus Val-11 and Lys-13) to the terminal carboxylic acid groups of Py in MWNT/Py surface was through the amine-carboxylic acid coupling chemistry, similar to that reported previously (denoted as MP11-amine$_{cov}$ film, Scheme 1).[4]

Scheme 1. Representation of the covalent immobilization of MP-11 on MWNT/Py modified HPG electrodes.

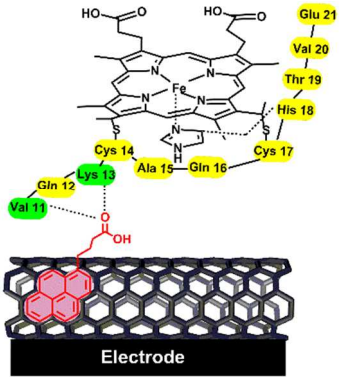

Figure S1 shows that the characteristic D and G bands of MWNT in the Raman spectrum were shifted to lower frequencies as a result of π-π interaction with Py molecules.[26,27] Thus, Raman

spectroscopy confirmed the π-π stacking of Py with surface MWNT coated on HPG electrodes. The formation of MP-11 films on the surface of MWNT/Py electrodes was confirmed by Fourier transform infrared spectroscopy operated in the attenuated total reflection mode (FTIR-ATR, Figures S2 and S3). The attachment of MP-11 to MWNT/Py units was also confirmed by surface morphological characterization using scanning electron microscopy (SEM, Figure 1), transmission electron microscopy (TEM, Figure S4), and energy dispersive spectroscopy (EDS, Figure S5).

For the SEM imaging, polished HPG surface was only partially modified with MWNT/Py assembly to allow the comparison of bare HPG surface and that coated with MWNT. As can be seen from Figure 1, the HPG surface showing platelet like features is covered by bundles of MWNT (Figure 1C and 1A). After the covalent attachment of MP-11 via amine groups, the MWNT/Py features were buried under the peptide film and resulted in a fiber-like texture (Figure 1B). The TEM images additionally supported the inferences obtained from SEM (Figure S4).[28] The presence of Fe and S (possibly from the MP-11 heme and cysteinyl sulfur, respectively) identified in the EDS analysis further confirmed the immobilization of MP-11 on the MWNT/Py modified electrodes (Figure S5).[29]

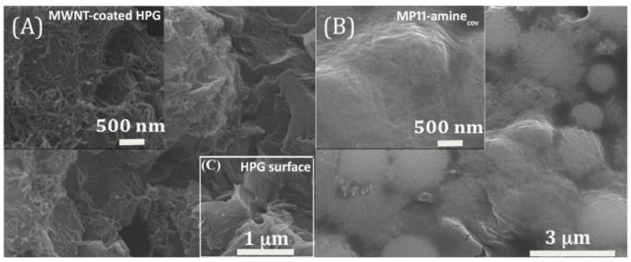

Figure 1. SEM images for **(A)** HPG/MWNT/Py and **(B)** MP11-amine$_{cov}$ films. **(C)** The image of a bare HPG surface displaying the texture of graphite flakes is shown for comparison.

Electrochemical studies were carried out to investigate the effect of MP-11 immobilization onto the pyrene linkers of MWNT/Py modified electrodes with respect to the electroactive MP-11 amount, direct electron transfer (ET) rates, and organic peroxide reduction currents. The cyclic voltammograms of the designed MP11-amine$_{cov}$ film in 0.1 M phosphate buffer saline (PBS), pH 7.4 displayed well-defined quasi-reversible redox peaks, and indicated the direct electron transfer between the heme cofactor of MP-11 and the MWNT/Py modified electrode surface (Figure 2A a). Similarly, the control MP-11 films coated on only HPG or HPG/Py or HPG/MWNT electrodes showed reversible voltammograms, however, at more positive $E^{o'}$ values due to the differences among the electrode surfaces that can possibly influence the MP-11 arrangements (Figure 2A b-d, Table 1). In the absence of immobilized MP-11, the MWNT/Py modified electrode alone or only the HPG electrode did not show any redox peaks (Figure 2B). This confirmed that the observed votlammetry in Figure 2A was of MP-11.

In fact, the large double layer capacitance of MWNT/Py modified HPG electrode indicates the feature of high surface area [Figure 2B(a)] and also suggests a supercapacitor property that has been shown for MWNT electrodes.[30] By plotting the charging current densities with scan rates for the HPG/MWNT/Py and bare HPG electrodes, we obtained the capacitance values of each electrode from the slopes of the resulting plots (Figure S6).[31] By this procedure, we determined that the capacitance of HPG/MWNT/Py was 1066 μF cm^{-2} and that of the polished HPG surface was 367 μF cm^{-2}. This indicates that the MWNT/Py modification on HPG electrode offered an ~ 3-fold greater electroactive surface area than the unmodified HPG electrode.

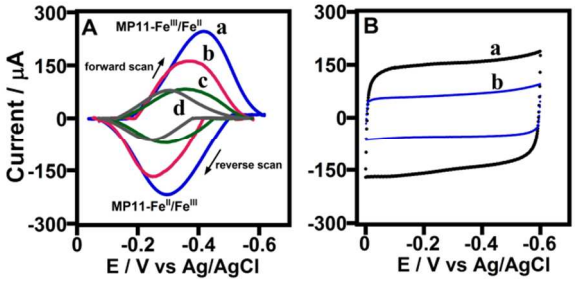

Figure 2. (A) Background subtracted cyclic voltammograms of **a.** MP11-amine$_{cov}$, **b.** MWNT-MP11 (EDC/NHS activated MWNT, but no pyrene linker), **c.** HPG/Py-MP11 with no MWNT, and **d.** HPG/MP11 with no Py and MWNT at 0.7 V/s in pH 7.4, PBS. **(B)** Cyclic voltammograms of **a.** MWNT/Py modified electrode and **b.** only HPG electrode with no MP-11 film.

The cathodic (E_{pc}) and anodic (E_{pa}) peak separation (ΔE_p) with increasing scan rate of the MP11-amine$_{cov}$ film was used to calculate the standard ET rate constant (k_s) by the Laviron's method (Figure S7 and details in Supporting Information).[32,33] A k_s value of 4.6 ± 0.2 s^{-1} was obtained for the designed MP11-amine$_{cov}$ film. The electroactive surface concentration (Γ) of MP11-amine$_{cov}$ film was calculated by integrating the area of the reduction or oxidation peak (since the peak current ratio was close to unity).[4,33,34] The MP11-amine$_{cov}$ film exhibited an ~ 2-fold higher electroactive coverage than the MWNT-MP11 film (EDC/NHS activated MWNT) without the pyrene linker [Figure 2A(b)], and ~ 3 to 4-fold enhancement in Γ than the films of HPG/Py-MP11 with no MWNT [Figure 2A(c)] and HPG/MP11 with no Py and MWNT [Figure 2A(d)] (Table S1). This property confirms the unique role of the pyrene linkers in facilitating higher density covalent immobilization of MP-11 and the associated large electroactive enzyme coverage in the MP11-amine$_{cov}$ film over other control films.

Furthermore, an 8-fold enhancement in Γ was obtained for the MP11-amine$_{cov}$ film when compared to a myoglobin film (-0.35 V vs Ag/AgCl, Table 1) attached similarly via surface amino groups on MWNT/Py modified electrodes (denoted as myoglobin-amine$_{cov}$, Table S1).[4] The electroactive coverage of MP-11 films on the modified electrodes suggests the formation of multilayer films, with a highly possible electron self-exchange phenomenon occurring between adjacent MP-11 heme centers.[21,23,33]

The electrocatalytic property of the MP11-amine$_{cov}$ film and other control films was investigated by monitoring the reduction of *tert*-Butyl hydroperoxide (t-BuOOH) to *tert*-Butanol (t-BuOH). The larger electroactive MP-11 in the MP11-amine$_{cov}$ film led to a 1.5 to 2-fold greater catalytic reduction current density of this film over control MP-11 films (Figure 3, Table 1). Thus, the enhancement effect of pyrene linkers on both the electroactive coverage and the electrocatalytic currents of immobilized MP-11 in the MP11-amine$_{cov}$ film can be understood. The currents were measured at the plateau region at -0.5 V vs Ag/AgCl, which is a high enough overpotential region, where the interfacial ET-rate is presumed to be not rate limiting.[10,11,33] The reduction currents were subtracted for the small background currents (≤ 5% of the catalytic current) from the respective electrodes with no immobilized MP-11 films (i.e., MWNT/Py, MWNT, HPG/Py, and only HPG; Fig. 4b illustrates the background reduction currents from the HPG/MWNT/Py electrode).

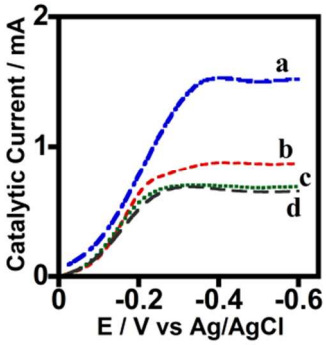

Figure 3. Electrocatalytic t-BuOOH (4.8 mM) reduction currents at 1000 rpm in PBS (pH 7.4), 25 °C, catalyzed by **a.** MP-amine$_{cov}$, **b.** MWNT-MP11 (EDC/NHS activated MWNT, but no pyrene linker), **c.** HPG/Py-MP11 with no MWNT, and **d.** HPG/MP11 with no Py and MWNT.

Table 1. Contribution of pyrene linker in enhancing the catalytic reduction currents of MP11-amine$_{cov}$ film over control films.

Enzyme film type	$E^{o'}$ (in V) vs Ag/AgCl	Catalytic Current Density (mA cm^{-2}) (at -0.5 V vs Ag/AgCl)
MP11-amine$_{cov}$	-0.36 (± 0.01)	7.5 ± 0.4
HPG/MP11 (no MWNT and Py-linker)	-0.28 (± 0.01)	3.4 ± 0.2
HPG/Py-MP11 (no MWNT)	-0.33 (± 0.01)	3.6 ± 0.1
HPG/MWNT- MP11 (no Py-linker)	-0.32 (± 0.03)	4.8 ± 0.2
myoglobin-amine$_{cov}$ (Ref. 4)	-0.35 (± 0.02)	4.1 ± 0.3

The t-BuOOH reduction currents catalyzed by the MP11-amine$_{cov}$ film versus the applied potential for increasing t-BuOOH concentrations are shown in Figure S8. The catalytic reduction current density (current divided by the electrode geometric area) versus the concentration of t-BuOOH present in solution is shown in Figure 4a. The small background reduction currents from the MWNT/Py electrodes with no MP-11 film are shown in Figure 4b.

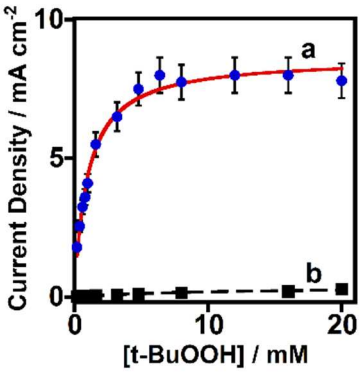

Figure 4. Catalytic current densities with t-BuOOH concentration at 1000 rpm for the designed **(a)** MP11-amine$_{cov}$ film and **(b)** MWNT/Py electrode in the absence of attached MP-11 in pH 7.4, PBS, 25 °C.

The designed MP11-amine$_{cov}$ film exhibited a high electrocatalytic activity with a current density of 7.5 mA cm^{-2} towards an organic peroxide reduction. The current density is greater by about 2–fold than the myoglobin-amine$_{cov}$ films.[4] This feature can be attributed to the small size of MP-11 heme peptide favoring high density surface concentration compared to the relatively large myoglobin protein. More interestingly, the apparent Michaelis-Menten constant (K_m^{app}) obtained from the Michaelis-Menten fit of reduction current density plot (Figure 4a) of the designed MP11-amine$_{cov}$ film (K_m^{app} = 1 mM) is 12-fold smaller than that observed by us for the myoglobin-amine$_{cov}$ film (K_m^{app} = 12 mM).[4] This suggests the stronger affinity of short MP-11 peptide by the designed covalent strategy over the similarly prepared large myoglobin protein film towards an organic peroxide substrate.

Conclusions

The results presented demonstrate that the π-π stacking of pyrene linkers with carbon nanotubes offers enhanced electroactive redox protein molecules and catalytic currents probably by retaining the innate electronic properties of MWNT and additionally by the presence of a large number of stacked pyrene units for high density, stable covalent enzyme immobilization. Furthermore, the findings above suggest a new potential direction in achieving high electrocatalytic activities of large, fragile, redox-center buried, or otherwise difficult to study metalloenzymes by mutating them into small catalytically active redox domains to effectively connect with electrodes.

Experimental

Materials. Equine heart microperoxidase-11 (MP-11) sodium salt, multiwalled carbon nanotubes (carbon >90% trace metal basis, outer diameter 10–15 nm, inner diameter 2–6 nm, length 0.1–10 µm, average wall thickness 5-15 graphene layers), 1-ethyl-3-[3-dimethylaminopropyl]carbodiimide hydrochloride (EDC), *tert*-Butyl hydroperoxide (t-BuOOH), 1-pyrenebutyric acid (Py), and N-hydroxysuccinimide (NHS) were purchased from Sigma and used as received. High purity graphite electrode disks (Grade: POCO EDM-4, Average Particle Size: <4 microns) were purchased from EDM Inc., MN, USA. All other chemicals used were high purity analytical grade.

Voltammetry. Voltammetric studies were carried out with a CHI 6017E workstation (Austin, TX, USA) at room temperature (25 °C) under a nitrogen atmosphere. A 3-electrode system consisting of a HPG electrode modified with MWNT/Py surface and attached with MP-11 as the working electrode, an Ag/AgCl (3 M KCl) reference electrode, and a platinum wire auxiliary electrode were used. Prior to surface modification, the HPG electrodes were sanded to expose a fresh surface by polishing on a SiC paper (P320 grit) followed by sonication in ethanol-water mixture and drying under nitrogen. The rotating disk voltammetry (RDV) was performed at a rotation rate of 1000 rpm using an EcoChemie Auto lab rotator system equipped with a motor controller unit (Metrohm Inc., USA).

Preparation of MP-11 films on MWNT/Py modified electrodes. The procedure to prepare MWNT/Py modified electrodes and covalent MP-11 immobilization is similar to our prior report.[4] In

brief, to the polished and cleaned surface of HPG electrodes (geometric area 0.2 cm^2), a 15 µL suspension of 1 mg/mL MWNT in dimethylformamide (DMF) was added and allowed to dry at room temperature. Following this, a 10-µL aliquot of 1-pyrenebutyric acid (Py, 10 mM) in DMF was added to each electrode. The electrodes were covered with a moisturized beaker (to avoid the Py solution from drying) and allowed for 1 hour to form the strong π-π stacked MWNT/Py assemblies. Then the electrodes were rinsed well in water.

For the selective covalent attachment of MP-11 through the free amine groups (Lys-13 and N-terminus Val-11), MWNT/Py electrodes were treated with a freshly prepared mixture of 0.35 M 3-[3- dimethylaminopropyl] carbodiimide hydrochloride (EDC) and 0.1 M N-Hydroxysuccinimide (NHS) to activate the carboxylic acid surface groups of Py by reacting for 10 min. The electrodes were rinsed in deionized water and subsequently 20 µL of MP-11 (1 mM in 0.1 M PBS) were added and incubated for 1 hour at 4 °C to obtain MP11-$amine_{cov}$ films.

Characterization of MP11-$amine_{cov}$ films. The characterization and surface morphological studies of the designed MWNT/Py modified electrodes and those attached with MP-11 films were carried out by Raman spectroscopy (Nicolet NXR FT-Raman module, Nd:YVO_4 laser, 0.2 W, resolution 4 cm^{-1}), Fourier transform infrared spectroscopy in the attenuated total reflection mode (Varian 800 FTIR, Scimitar Series), scanning electron microscopy (SEM), energy dispersive spectroscopy (EDS, FEI Quanta 600 field emission gun ESEM with Evex EDS and HKL EBSD) and transmission electron microscopy (TEM, JEOL JEM-2100).

Acknowledgements

Financial support by Oklahoma State University is greatly acknowledged. We thank Dr. Smita Mohanty and Dr. Jose Soulages for helpful discussions.

Notes and references

Department of Chemistry, Oklahoma State University, Stillwater, OK, USA-74078.
*E-mail: gopan.krishnan@okstate.edu

Electronic Supplementary Information (ESI) available: Figures S1-S8 detailing the spectroscopic and microscopic characterization, capacitive current versus scan rate plots of HPG/MWNT/Py and only HPG, potential versus logarithmic scan rate, and electrocatalytic voltammograms. See DOI: 10.1039/c000000x/

1 C. Leger and P. Bertrand, *Chem. Rev*., 2008, **108**, 2379–2438.
2 A. Walcarius, S. D. Minteer, J. Wang, Y. Lin and A. Merkoci, *J. Mater. Chem. B,* 2013, **1**, 4878- 4908.
3 E. S. Redeker, D. T. Ta, D. Cortens, B. Billen, W. Guedens and P. Adriaensens, *Bioconjugate. Chem*., 2013, **24**, 1761–1777.
4 C. Walgama and S. Krishnan, *J. Electrochem. Soc.,* 2014, **161**, H47-H52.
5 I. Willner and E. Katz, *Angew. Chem. Int. Ed.,* 2000, **39**, 1180−1218.
6 E. Lojou, *Electrochim. Acta,* 2011, **56**, 10385-10397.
7 M. Calvaresi and F. Zerbetto, *Acc. Chem. Res.,* 2013, **46**, 2454–2463.
8 R. J. Chen, Y. Zhang, D. Wang and H. Dai, *J. Am. Chem. Soc.,* 2001, **123**, 3838-3839.
9 J. J. Gooding, R. Wibowo, J. Q. Liu, W. R. Yang, D. Losic, S. Orbons, F. J. Mearns, J. G. Shapter and D. B. Hibbert, *J. Am. Chem. Soc.,* 2003, **125**, 9006–9007.
10 G. Göbel and F. Lisdat, *Electrochem. Commun.,* 2008, **10**, 1691-1694.
11 S. Krishnan and F. A. Armstrong, *Chem. Sci.,* 2012, **3**, 1015–1023.
12 L. Halamkova, J. Halamek, V. Bocharova, A. Szczupak, L. Alfonta and E. Katz, *J. Am. Chem. Soc*., 2012, **134**, 5040−5043.
13 M. Wang, F. Zhao, Y. Liu and S. Dong, *Biosens. Bioelectron*., 2005, **21**, 159-166.
14 T. Mashino, S. Nakamura, M. Hirobe, *Tetrahedron Lett.* 1990, **31**, 3163-3169.
15 E. Ryabova and E. Nordlander, *Dalton Trans*., 2005, **7**, 1228–1233.
16 T. L. Poulos, *J. Biol. Inorg. Chem*., 1996, **1**, 356–359.
17 F. Mazzei, G. Favero, F. Frasconi, A. Tata and F. Pepi, *Chem. Eur. J.,* 2009, **15**, 7359–7367.
18 E. Katz and I. Willner, *Langmuir* 1997, **13**, 3364-3373.
19 T. Lotzbeyer, W. Schuhmann, E. Katz, J. Falter and H.-L. Schmidt, *J. Electroanal. Chem*., 1994, **377**, 291–294.
20 T. Lotzbeyer, W. Schuhmann and H.-L. Schmidt, *J. Electroanal. Chem*., 1995, **395**, 341–344.
21 T. Ruzgas, A. Gaigalas and L. Gorton, *J. Electroanal. Chem*., 1999, **469**, 123–131.
22 Y. Liu, M. Wang, F. Zhao, Z. Guo, H. Chen and S. Dong, *J. Electroanal. Chem*. 2005, **581**, 1–10.
23 A. Yarman, T. Nagel, N. Gajovic-Eichelmann, A. Fischer, U. Wollenberger and F. W. Scheller, *Electroanalysis,* 2011, **23**, 611-618.

24 C. Renault, C. P. Andrieux, R. T. Tucker, M. J. Brett, V. Balland and B. Limoges, *J. Am. Chem. Soc.,* 2012, **134**, 6834−6845.
25 S. Tian, Q. Zhou, Z. Gu, X. Gu, L. Zhao, Y. Li and J. Zheng, *Talanta,* 2013, **107**, 324–331.
26 Y. Zhang, S. Yuan, W. Zhou, J. Xu and Y. Li, *J. Nanosci. Nanotechnol.,* 2007, **7**, 2366.
27 Q. Yang, L. Shuai, J. Zhou, F. Lu and X. Pan, *J. Phys. Chem. B,* 2008, **112**, 12934.
28 D. Zhang, L. Zhang, L. Shi, C. Fang, H. Li, R.Gao, L. Huang and J. Zhang, *Nanoscale*, 2013, **5**, 1127.
29 D. Zhang, L. Zhang, C. Fang, R. Gao, Y. Qian, L. Shi and J. Zhang, *RSC Adv*., 2013, **3**, 8811.
30 E. Frackowiak, K. Metenier, V. Bertagna and F. Beguin, *Appl. Phys. Lett.,* 2000, **77**, 2421.
31 D. Svedruzic, J. L. Blackburn, R. C. Tenent, J.-D. R. Rocha, T. B. Vinzant, M. J. Heben and P. W. King, *J. Am. Chem. Soc.,* 2011, **133**, 4299.
32 E. Laviron, *J. Electroanal. Chem*., 1979, **101**, 19-28.
33 S. Krishnan, A. Abeykoon, J. B. Schenkman and J. F. Rusling, *J. Am. Chem. Soc.,* 2009, **131**, 16215.
34 S. Krishnan and C. Walgama, *Anal. Chem.* **2013**, *85*, 11420.